

Lateral adsorption geometry and site-specific electronic structure of a large organic chemisorbate on a metal surface

A. Kraft,¹ R. Temirov,¹ S. K. M. Henze,¹ S. Soubatch,¹ M. Rohlfing,^{1,2} and F. S. Tautz^{1,*}

¹*School of Engineering and Science, International University Bremen, 28725 Bremen, Germany*

²*Fachbereich Physik, Universität Osnabrück, 49074 Osnabrück, Germany*

(Received 31 May 2005; revised manuscript received 3 February 2006; published 7 July 2006)

A combined study of scanning tunneling microscopy (STM) and density functional theory (DFT) reveals that 3,4,9,10-perylene-tetracarboxylic-dianhydride (PTCDA) adsorbs on Ag(111) at bridge sites in two nonequivalent orientations, one nearly aligned with the $[10\bar{1}]$ substrate axis and the other 18° misaligned. Site-specific spectroscopy reveals that molecules in the two configurations exhibit subtle differences in their electronic structure. DFT-based STM simulations trace these back to the influence of distinct local adsorption geometries on the chemical molecule-substrate and molecule-molecule interactions.

DOI: [10.1103/PhysRevB.74.041402](https://doi.org/10.1103/PhysRevB.74.041402)

PACS number(s): 68.37.Ef, 68.43.Bc, 68.43.Fg, 73.20.Hb

The mechanisms controlling the ordering of large organic molecules on metal surfaces are currently investigated intensively. The chemical interaction of the adsorbate with the metal is a key issue, as it determines equilibrium interface structures as well as kinetic processes that govern the ordering process. Two-dimensional ordered layers of large π -conjugated adsorbates on metals display a rich variety of incommensurate, coincident, and commensurate structures,¹ calling for a detailed analysis of the chemical and/or physical adsorbate-substrate bonding and its balance with intermolecular interactions. Ultimately, this demands experiments at the single molecule level, because nonequivalent adsorption sites with distinct properties often coexist in a single phase of a large adsorbate.

Here we present a detailed study of bonding and structure of a complex adsorbate at the single molecule level. Our model system is the interface of the prototypical 3,4,9,10-perylene-tetracarboxylic-dianhydride (PTCDA) molecule with the Ag(111) surface. On Ag(111), PTCDA forms flat lying commensurate monolayers arranged in a herringbone pattern^[2] with a surface unit cell containing two molecules in well-defined but nonequivalent adsorption configurations. We precisely determine the two different adsorption geometries by high-resolution imaging, and we investigate by scanning tunneling spectroscopy (STS) their influence on the respective electronic structures. From this analysis we can clearly differentiate the influence of molecule-substrate interactions on the properties of the adsorbate from the influence of molecule-molecule interactions, and thus develop a comprehensive understanding of this model chemisorbate.

PTCDA is a large π -conjugated organic model molecule for organic epitaxy³ and complex chemisorption phenomena.^{4,5} Some details of the adsorption, e.g., the geometric distortion of the molecules, have already been revealed.⁴ Site-specific properties, however, have been inevitably missed so far by standard spectroscopic or structural techniques, since they average over the two nonequivalent molecules in the monolayer.

Experiments have been performed with a scanning tunneling microscope at 10 K. The Ag(111) surface was prepared by sputter-anneal cycles. PTCDA was evaporated at 720 K onto Ag(111) at 300 K, followed by annealing at 550 K. At

submonolayer coverage, the surface exhibits large PTCDA islands and areas in which the clean silver surface is exposed.²

We start with the adsorption geometry. Determining bonding sites of large adsorbates on metal surfaces is an experimental challenge. Direct site imaging in scanning tunneling microscopy (STM) is usually impossible because appropriate tunneling conditions for substrate and adsorbate differ too much.^{6,7} Moreover, the achievable resolution on the adsorbate is often reduced by the molecule-substrate interaction,⁸ which tends to exclude the most interesting (since strongly interacting) systems from study. Here we show that by adjusting the bias voltage online just before the tip reaches a PTCDA island, it is possible to resolve both the substrate lattice and the internal molecule structure in one image, cf. Fig. 1(a).

Images like Fig. 1(a) allow the determination of molecular adsorption sites. To this end, equidistant lattice lines are fitted to the Ag atoms in the left part of the image,¹¹ under the additional constraint that these lines must be commensurate with the PTCDA superstructure.^{2,3} If the so determined Ag lattice [Fig. 1(a) inset] is extended into the PTCDA region [Fig. 1(b)], (Ref. 12), one finds by inspection that the centers of all molecules are located at or close to bridge sites of the Ag surface. The error of this assignment by inspection is ± 0.7 Å. It is possible, however, to reduce this by a more sophisticated analysis (see below). Figure 1(b) also shows that molecules of type A are almost perfectly aligned with the $[10\bar{1}]$ Ag lattice direction, while type-B molecules are rotated by $18 \pm 2^\circ$ with respect to $[0\bar{1}1]$.

To record high-resolution images like Fig. 1(a) we have purposely picked up a molecule by a defined protocol. Accidental changes in the tip configuration occurring at the voltage step could therefore lead to a systematic lateral offset between both parts of the image, invalidating the adsorption site determination. However, repetition of the experiment displayed in Fig. 1(a) always led to the same Ag/PTCDA lattice registry. Moreover, the thus determined adsorption site is confirmed by density-functional theory (DFT) theory, as we will show now.

Calculations have been carried out with SIESTA (Refs. 4, 13, and 14). The Ag substrate is modeled by three atomic

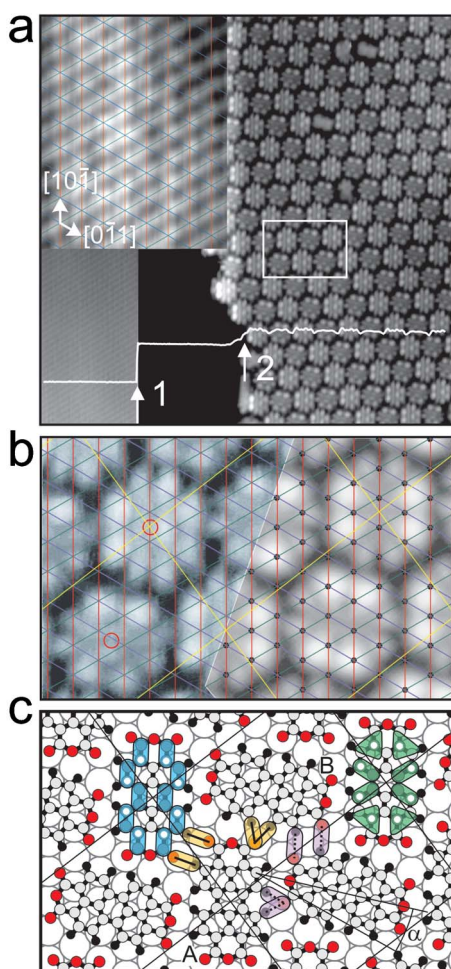


FIG. 1. (Color online) (a) STM micrograph ($186 \text{ \AA} \times 186 \text{ \AA}$): Ag(111) atomic structure (left) and PTCDA/Ag(111) (right) at 10 K. Scan direction: bottom to top (fast), left to right (slow). Marked scan line (arrow 1): scanning parameters were changed from $U = -10 \text{ mV}$ (left) to $U = -1.5 \text{ V}$ (right) at constant $I = 6.6 \text{ nA}$ (tip retraction from ~ 3.0 to 7.8 \AA). Inset: $27 \text{ \AA} \times 21 \text{ \AA}$ region from (a) including fitted lattice lines, cf. text. (b) Image section as indicated by the white frame in (a), including Ag grid lines (red, green, blue/shades of gray). Experimental (left) and simulated (right) (*s*-tip) images, the latter inserted into the experimental image with maximum correlation (cf. text). Thin yellow (light gray) lines: PTCDA/Ag(111) supercell (Ref. 2). Red (dark gray) circles (radius 0.7 \AA): molecule centers. Black dots: Ag positions underneath the simulated image. (c) Ball-and-stick model corresponding to (b), showing DFT-optimized adsorption sites. Schematic representations of free molecule LUMO and HOMO in blue (left) and green (right). White dots give centers of corresponding lobes. Shortest O-H bridges are shown as solid (O on type A) and dotted lines (O on type B); details in text.

layers.¹⁵ The adsorption site is determined by total energy minimization. To this end, a monolayer with the correct superstructure is placed on the Ag lattice and fully relaxed. While internal molecular bond lengths, vertical positions of individual atoms, the overall height of the molecule, and the molecular orientations inside the supercell easily converge into a total energy minimum, the relaxation of the lateral registry is much slower. Therefore, the layer was placed in

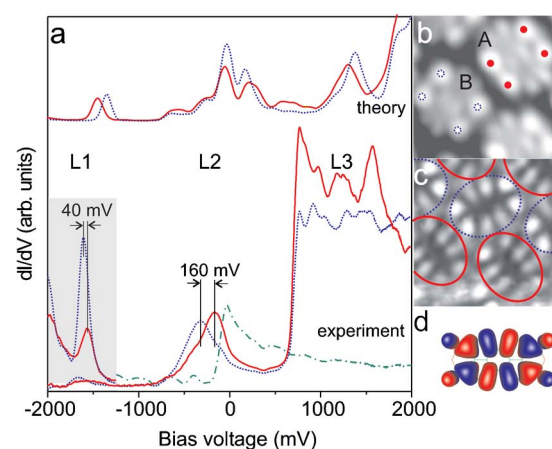


FIG. 2. (Color online) PTCDA/Ag(111): (a) Experimental (background-subtracted) and simulated dI/dV spectra, recorded on molecules of type A (red, full line) and B (blue, dashed line), cf. dots in (b). Tip height during STS: approx. 7.5 \AA . Experimental spectra recorded with sensitized tip (Ref. 16) are shaded. Green (dash-dotted) spectrum: Ag(111). (c) dI/dV image recorded in the left flank of L1 ($I = 1.8 \text{ nA}$, modulation $288 \text{ Hz}/20 \text{ meV}$). (d) Calculated free molecule HOMO.

six different positions and orientations with respect to the Ag lattice.¹⁴ The configuration in which both molecules are located on bridge sites, one nearly aligned to $[10\bar{1}]$ (2° off – type A), the other 17° misaligned versus $[01\bar{1}]$ (type B), has the lowest energy.¹⁴ This structure fully agrees with experiment.

Having established the two distinct adsorption geometries [Fig. 1(c)], we now analyze their site-specific electronic properties. Figure 2(a) displays experimental and simulated STS spectra.¹⁴ We observe a resonance (L1) at $\sim -1.7 \text{ eV}$, a broader level (L2) at $\sim -0.3 \text{ eV}$ (crossing the Fermi level E_F), and a continuum L3 above E_F (Ref. 16). L1 corresponds to the highest occupied molecular orbital (HOMO) of free PTCDA, as comparison of its spectroscopic image with the calculated free molecule HOMO [Figs. 2(c) and 2(d)] and a spectral decomposition of the corresponding feature in the simulated STS prove. Judging from its sharpness, L1 mixes less with metal states than L2, which is derived from the lowest unoccupied molecular orbital (LUMO) of free PTCDA. Hence we can conclude that chemical substrate bonding is mainly effected by the LUMO, which forms the bonding hybrid L2 with metal states and accepts charge from the metal, with little back donation from the molecule to the metal. We note the strong reduction of the L1-L2 gap if compared to the optical HOMO-LUMO gap of bulk PTCDA (2.3 eV) (Ref. 17) or the transport gap (3.8 eV) (Ref. 18).

Incidentally, the very different behavior of LUMO (strongly mixing and broad) and HOMO (rather sharp) is related to the spatial properties of their respective wave functions [cf. Fig. 1(c)]: For A molecules, the lobes of the HOMO align with interstitial positions of the substrate, whereas the four outer lobes of the LUMO sit above substrate atoms, thus facilitating orbital mixing.

Most importantly, experimental spectra in Fig. 2 reveal site-specific differences for L1 and L2. For L2 this is not too

surprising, since this orbital is implicated in the substrate bond and therefore affected directly by the different bonding orientation. However, it is not clear why L1 with its smaller participation in the chemisorption bond is also affected. A DFT analysis shows that this is primarily a result of intermolecular interactions: Turning to Fig. 1(c), we find that H bonds between two molecules of type A have a length of 2.36 Å (solid lines), while equivalent bonds between type-B molecules have a length of 2.55 Å (dotted lines). Bonds between O atoms on A and H atoms on B have a length of 2.15 Å (solid lines), while bonds between O on B and H on A have a length of 2.04 Å (dotted lines). The 1° distortion of the PTCDA unit cell from rectangular shape (enforced by substrate commensurability²) is the origin of these subtle modifications. In the rectangular unit cell of an undistorted herringbone layer both molecules and their H bonds would be fully equivalent.

These differences in the O-H bond distances are responsible for an upward shift by 120 meV of the A-type L1 as compared to the B-type L1. The interaction with the Ag substrate, on the other hand, causes a L1 shift of similar size in the opposite direction (resulting from the different lattice alignments of A and B). In our DFT-LDA calculation, the latter effect overcompensates the splitting due to the O-H bonds, yielding a different order of type-A and type-B L1 features than found in experiment, where the type-A L1 is 40 meV *above* type-B L1. The balance of these two effects may simply be too subtle to be fully described by our DFT-LDA calculations, which show a tendency to overbond.¹⁴ Nonetheless, the observed ordering of L1 levels, together with the clear trends in the calculation, indicates that the intermolecular interaction is the dominant cause determining the relative energy positions of the L1 levels of both types of molecules.

The different bonding also shows up as different image contrast. Such contrast differences are apparent in Fig. 1, where the aligned molecule has sharper internal contrast. On the basis of the calculated structure (but with the molecule constrained to the experimental height¹⁵), we have simulated STM images, using a Tersoff-Hamann approach,¹⁹ for quantitative comparison with experiment. To this end, the energy-resolved local density of states at the tip position, i.e., several angstrom above the molecules, is calculated by decomposing each wave function close to the molecular layer (where the DFT wave functions are reliable) into plane waves and extrapolating the latter into the vacuum. From all plane-wave components, the wave function can be evaluated at any selected height, giving the information required to obtain the tunneling current for various tip symmetries and heights²⁰ and to evaluate constant current z trajectories.

Figure 3 shows measured and calculated STM images at characteristic tunneling conditions. The agreement between experiment and theory is very good for a broad range of tip-sample distances, sample biases, and tips. In the bias range from -1.0 to 0.5 V the LDOS is dominated by the LUMO-like L2 (cf., also, Figs. 1 and 2), while at larger negative biases a V-like feature corresponding to the HOMO-like L1 [Figs. 2(c) and 2(d)] becomes visible [Figs. 3(b) and 3(c)]. The experimental images in Figs. 3(c)–3(e) show contrast between the two inequivalent molecules: For

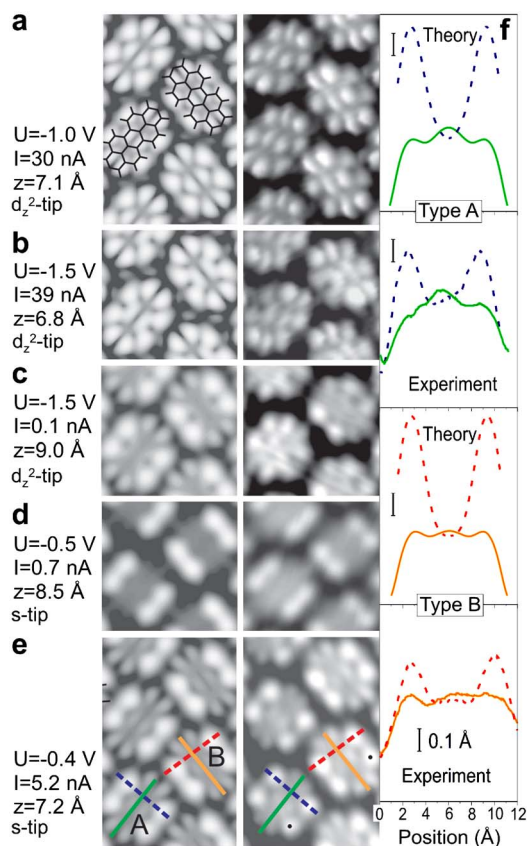


FIG. 3. (Color online) PTCDA/Ag(111): (a–e) Experimental (right) and calculated (left) STM images (23 Å width). Experimental tip heights determined from current-distance curves. (f) Experimental and simulated corrugation as indicated by corresponding bars in (e).

increasing tip-sample distances, the internal structure for the misaligned molecule is lost more rapidly [Fig. 3(c)], showing that image contrast is determined by both molecule *and* substrate. In the simulation this contrast difference is also present [cf., for example, solid profiles in Fig. 3(f)], but it is much harder to make out in the simulated topographs [Figs. 3(c)–3(e)]. Small differences between A and B molecules in the metal-to-molecule charge transfer, which is responsible for the contrast difference, are difficult to resolve because of quantum confinement effects in the three-layer slab.

Finally, simulated images can be used to refine the adsorption site determination. Figure 1(b) shows a direct comparison of a measured STM image (left) and a calculated one (right). The calculated image has been inserted with maximum image correlation into the experimental one by a subpixel mathematical correlation routine. In this way the measured and simulated molecules are brought into registry. Because the simulated image has the positions of Ag atoms [black dots in Fig. 1(b)] corresponding to exact bridge adsorption attached to it, any deviation between the experimental Ag grid and the Ag positions in the calculated image gives a measure of the observed molecules' deviation from the experimental bridge site. We find this error to be ± 0.2 Å and can finally assign both molecules to a bridge site.

In summary, we have resolved the lateral interface struc-

ture of an archetypal organic chemisorbate and its electronic structure by high-resolution imaging and spectroscopy in conjunction with DFT. Conventional methods of adsorption site determination, since they are based on tip-induced manipulations, are limited to solitary molecules⁷ or molecules at the border of adsorbate islands,²¹ which are generally not representative of molecules within islands. In contrast, the method introduced here is also applicable to molecules inside compact layers. The very different behavior of the LUMO (strongly mixing, broad, metallic) and the HOMO (rather sharp) on adsorption can be understood from the local adsorption geometry. For the two inequivalent monolayer

molecules, both states exhibit subtle differences: For the bonding LUMO, this variation results directly from different alignment with the Ag substrate, while for the weaker bonding HOMO the influence of the substrate is mediated by the distortion of the unit cell from orthogonality. This demonstrates a delicate interplay between adsorbate–adsorbate and adsorbate–substrate interactions for this chemisorbate.

We thank S. Zoepfel of Createc GmbH for helpful discussions and experimental support. This work was funded by the Deutsche Forschungsgemeinschaft (DFG).

*Corresponding author. Email address: s.tautz@iu-bremen.de

¹S. R. Forrest, *Chem. Rev.* (Washington, D.C.) **97**, 1793 (1997).

²K. Glöckler *et al.*, *Surf. Sci.* **405**, 1 (1998).

³L. Kilian, E. Umbach, and M. Sokolowski, *Surf. Sci.* **573**, 359 (2004).

⁴A. Hauschild *et al.*, *Phys. Rev. Lett.* **94**, 036106 (2005); **95**, 209602 (2005); R. Rurali *et al.*, *ibid.* **95**, 209601 (2005).

⁵M. Eremtchenko, J. A. Schaefer, and F. S. Tautz, *Nature* (London) **425**, 602 (2003).

⁶G. Meyer, S. Zöphel, and K.-H. Rieder, *Phys. Rev. Lett.* **77**, 2113 (1996).

⁷J. Lagoute, K. Kanisawa, and S. Fölsch, *Phys. Rev. B* **70**, 245415 (2004).

⁸Orbital imaging works much better if the molecule–substrate interaction is negligible (Ref. 9) or small (Ref. 10).

⁹J. Repp *et al.*, *Phys. Rev. Lett.* **94**, 026803 (2005).

¹⁰X. Lu *et al.*, *Phys. Rev. B* **70**, 115418 (2004).

¹¹A Tersoff–Hamann analysis on the basis of a density-functional calculation for Ag(111) reveals that, irrespective of tip (*s* or *d_z* symmetry), Ag atoms are imaged as protrusions.

¹²Due to nonideal calibration of the piezos, the resulting Ag lattice lines deviated slightly from hexagonality. The image presented in Fig. 1(a) has been corrected to show hexagonal symmetry.

¹³P. Ordejón, E. Artacho, and J. M. Soler, *Phys. Rev. B* **53**, R10441 (1996); E. Artacho *et al.*, *J. Phys.: Condens. Matter* **14**, 2745 (2002).

¹⁴DFT was performed in local density approximation (LDA) and generalized gradient approximation (GGA) with standard double-zeta basis orbitals including polarization for Ag and H, and triple-zeta orbitals including polarization for O and C. Both

LDA and GGA yield the bridge-bridge adsorption geometry [aligned with the Ag(1 $\bar{1}$ 0) direction] as adsorption site [binding energy 5.98 eV or 150 meV/unit cell (LDA/GGA)]. Additional tested sites: top/bridge (i.e., center of molecule 1 on top of an Ag atom, center of molecule 2 on a Ag–Ag bridge position), bridge/top, bridge/bridge with 60° misalignment, hollow/somewhere (“somewhere” means a non-high-symmetry position near a top position), and another hollow/somewhere combination. Within LDA, the corresponding adsorption energies amount to 5.60, 4.92, 4.94, 5.30, and 5.38 eV (GGA: 0.14, 0.05, 0.01, 0.09, and 0.06 eV) per unit cell. LDA/GGA yield a vertical adsorption height of 2.70 Å/3.40 Å for the central carbon atom, while the experimental average carbon height is 2.86±0.01 Å (Ref. 4). For the STM-simulations in Figs. 2 and 3, the molecule was fixed at the experimental height.

¹⁵Ag slab relaxation from ideal bulk positions is <0.05 Å.

¹⁶Due the intrinsic asymmetry between negative and positive bias, the experimental spectra recorded with the standard tip (W dipped into Ag) exhibit very weak (but reproducible) signals at the position of L1. To achieve optimum conditions for spectroscopy of L1, a less stable sensitized tip (the same as that used for high-resolution spatial imaging) was employed. For L2 and L3, a silver tip, which gives worse spatial resolution, yields better reproducibility for spectra.

¹⁷H. Proehl *et al.*, *Phys. Rev. Lett.* **93**, 097403 (2004).

¹⁸E. V. Tsiper *et al.*, *Chem. Phys. Lett.* **360**, 47 (2002).

¹⁹J. Tersoff and D. R. Hamann, *Phys. Rev. B* **31**, 805 (1985).

²⁰C. J. Chen, *Phys. Rev. Lett.* **65**, 448 (1990).

²¹M. Böhlinger *et al.*, *Surf. Sci.* **419**, L95 (1998).